5-20-2005

Nanomaterials Self-Assembly Driven by Beta-Amyloid Peptides

Maria Elena Tanase
University of New Orleans

NANOMATERIALS SELF-ASSEMBLY DRIVEN BY BETA-AMYLOID PEPTIDES

A Thesis

Submitted to the Graduate Faculty of the
University of New Orleans
in partial fulfillment of the
requirements for the degree of

Master of Science
in
The Department of Chemistry

by

Maria Tanase

BS Babes-Bolyai University 1992
MBA Babes-Bolyai University 1999

May, 2005

Acknowledgements

First I would like to thank my research advisor, Professor Paul Hanson, for his help, advice and guidance throughout my graduate research. I am very grateful to my committee members, Professor John B. Wiley and Professor Mark L. Trudell for useful discussions and constructive comments.

I would like to thank Dr. Guijun Wang for the help in using the optical light microscope.

I am grateful to Daniela Caruntu and Larisa Radu for their help in taking electronic microscope images.

I would like to thank my parents and my husband who encouraged and supported me during all this period.

Table of Contents

Abstract

Nanomaterials such as gold nanowires and gold nanoparticles were self-assembled with several peptides derived from beta-amyloid peptide. The peptides propensity to form fibrilar structures was exploited. The products obtained by aggregation of the peptides with the nano materials were studied using HPLC, UV-vis spectroscopy, TEM and optical light microscopy.

Chapter 1

Introduction

1.1 Nanoscale assembly

The nanomaterials field has emerged lately as a very promising research area, with applications in nanotechnology, biotechnology, medicine, etc. Nanoscale structured materials have dimensions of nanometer order (0.1-100 nm), and their properties depend strongly on their microstructure (the arrangement of the atoms and the chemical composition).

Two approaches are commonly used to construct nanomaterials: the “top-down” approach, where large building blocks are manipulated to afford smaller size building blocks that can be further assembled. Photolithography makes use of this approach to obtain two-dimensional structured materials. The other way to manufacture-synthesize nanomaterials is the “bottom-up” approach, where molecular entities are assembled to afford materials with nanometer length scale and with an ordered structure. The molecular self-assembly process is driven by spontaneous association of the building blocks, also known as “Brownian assembly”. Various organic molecules such as thiols, can spontaneously attach to substrates like gold to form ordered layer [1], this process being a self-assembling one.

Molecules can be designed to self assemble in a controlled manner to create a structure with predictable properties. Nanobuilding blocks with various shapes have been synthesized to date. Nanospheres [2], nanorods [3], nanocubes [4], nanoplates [5] are synthesized to be used in areas like photonics, electronics, chemical and biological

sensors, and their manipulation into functional materials and devices is a permanent challenge for nanotechnology.

1.2 Nanoscale Assembly Importance

Very often molecular self assemblies are inspired by nature. The living cells are perfect examples for how proteins and lipids are assembled to perform special functions and to respond to various stimuli. Proteins and peptides are intensively studied, and knowing their functions, folding and properties helps in using them as building blocks in a "bottom-up" manner. Another advantage of using proteins or peptides as self-assembling entities is that the bulk properties of the material obtained in this fashion are similar to the properties of the individual component blocks. The self-assembling process is a dynamic process driven by weak noncovalent interactions (hydrogen bonding, electrostatic and/or hydrophobic interactions) and/or metal coordination.

De novo design of proteins and peptides aims to self-assemble proteinaceous monomeric blocks of small size that may have, besides their affinity to self-assemble, functional groups incorporated. Current research is exploring the fabrication of nanostructures with applications in medicine [8, 29] or areas such as photonics and electronics [30], chemical and biological sensors, energy storage [31], and catalysis [32].

1.3 Progress Made Toward Obtaining Nanoscale Materials through Self-assembling Processes

Naturally occurring proteins with known assembling properties are used as starting points to synthesize structures with different morphologies. Self-assembling of biological materials with inorganic compounds is called biomineralization. The Hartgerink group [6] self assembled a fibril forming peptide into nanofibers which were

reversibly cross linked and then, by direct mineralization with hydroxyapatite and varying the pH, the long axes of the fibers were aligned with the crystallographic axes of the hydroxyapatite in a manner similar to the alignment of the collagen fibrils and hydroxyapatite crystals in bone.

The chemical synthesis of peptides can be very easily performed and the peptides can be designed to have a desired pattern or it is possible to attach in specific points amino acids or molecules with functional groups that will allow a further attachment or assembly. Peptides can be synthesized to adopt well defined supramolecular structures such as nanotubes [7]. Metallization of peptide nanotubes [8] can be achieved and then, by enzymatic means, the peptide that served as a scaffold can be eliminated to obtain nanowires with smaller diameters than the peptide used to drive the metal wires formation.

In spite of the advantages of using proteins and peptides as building blocks, a major draw-back is their fragility when exposed to environmental conditions, such as highly acidic or basic conditions, high temperature, etc. The enzymatic degradation is also a continuous challenge for “in vivo” applications, but, by carefully controlling it, it can be encompassed [9].

Our hypothesis is that nanoscale assembly can be driven by biological systems. In this project, the synthesized peptides are linked to nanowires or gold nanoparticles with different sizes by Au-S covalent bonds. The rate of beta-amyloid peptides aggregation with the gold nanowires was observed using HPLC and Transmission Electron Microscope. The rate of beta amyloid peptides aggregation with the gold nanoparticles

was monitored by kinetic spectrophotometric measurements and the products were visualized by TEM and optical light microscopy.

Chapter 2

Beta-amyloid Peptides

2.1 Introduction

Amyloid related diseases, such as Alzheimer's disease, Huntington's disease, type 2 diabetes, prion diseases, are a result of protein misfolding. In all stages of these diseases, amyloid fibrils are formed as a result of a self-assembly process. It is known that protein folding into fibrils is dictated by the protein sequence but, the appearance of the self assembled amyloid fibrils might be also influenced by other factors, like the interaction with cellular components (apolipoprotein E, glycoproteins, glycans, etc.) or metals (Ca, Zn)[27].

The amyloid fibril forming process is termed amyloidosis and it generally describes the aggregation of proteins or peptides in the brain or body. These aggregates can be soluble or insoluble and the accumulation of the insoluble fibers or fibrils generates the insoluble amyloid plaques. Several peptides and proteins with diverse amino acid sequences exhibit this property [28]. Two of the peptides responsible for these deposits which were intensively studied because their involvement in protein misfolding diseases are a 40- and a 42- amino acids residue peptide called beta-amyloid [27]. The beta-amyloid peptides have the following sequences:

a) The 40 amino acid sequence

NH_2- DAEFRHDSGYEVHHQKLVFFAEDVGSNKGAIIGLMVGGVV-COOH

b) The 42 amino acid sequence

NH_2- DAEFRHDSGYEVHHQKLVFFAEDVGSNKGAIIGLMVGGVVIA-COOH

The beta-amyloid peptide showed, when studied by transmission electron microscope, its ability to form fibrils with distinct morphologies (twisted or parallel assemblies of smaller scale fibrils, proto-fibrils). Recently, by using electron microscopy and solid state NMR techniques, R. Tykco group [10] demonstrated that the predominant structure of the formed fibrils can be controlled by variations in fibril growth conditions and moreover, that the molecular structure and the morphology of the fibrils are self-propagating when the fibrils grow from preformed seeds. They showed also that different morphologies of the fibrils have different toxicities in neuronal cell cultures, results that emphasize, once more, the importance of understanding the mechanism of amyloid fibrils formation.

2.2 Beta-amyloid Short Sequences

In order to understand what drives the beta-amyloid fibrils formation, the 1-40 and 1-42 sequences were studied truncated, using various techniques and approaches. It was determined by Tjernberg L. [11] that the shortest fragment of 1-40/42 peptide influencing the binding abilities of beta amyloid is the sequence 16-20 (**KLVFF**). This fragment was found to be soluble, unable to form fibrils by itself, but it showed a pronounced ability to influence fibril formation by binding to longer sequences derived from beta amyloid peptide.

Segments of beta-amyloid fibrils forming peptides derived from the beta-amyloid 1-42 peptide were studied by several groups, such as: Tycko [12], Langen [13], Nordstedt [14], Nussinov [15], Thirumalai [16]. The sequence 16-22 (**KLVFFAE**) was given a special attention because its importance in the amyloid fibrils genesis. The sequence 16-22 is the

shortest sequence that forms fibrils. Moreover, it was shown that mutations within this sequence determine the loss of the peptide ability to form fibrils [16].

In our experiments we tried to exploit the tendency of sequence 16-22 to form amyloid fibrils and we attached cysteine at the N-terminus at two of the sequences. The cysteine was attached to enable the binding to various gold containing nanoparticles and nanowires. We synthesized the sequences:

a) beta-amyloid 16-20 (bamc16-20) **C-K-L-V-F-F**

b) beta-amyloid 16-22 (bam 16-22) **K-L-V-F-F-A-E**

c) beta-amyloid 16-22 (bamc16-22) **C-K-L-V-F-F-A-E**

The letters correspond to:

C- cysteine; K- lysine; L- leucine; V- valine; F- phenylalanine; A- alanine; E- glutamic acid.

The sequences are fragments from the beta-amyloid peptide containing the amino acids between position 16 through 20 and 22 respectively. To allow a reaction with the gold nanoparticles we attached a cysteine amino acid in position 15. The sequences were chosen because the first one is known to enhance the fibril formation. The second sequence is the shortest amyloid fibrils forming peptide derived from the 1-42 beta-amyloid peptide. The third sequence differs from the second one with only an additional cysteine that will function as a linker between the peptide and the gold nanoparticles.

2.2.1 Synthesis of Beta-amyloid Short Sequences

The peptides were synthesized using an Fmoc procedure (Fmoc stands for 9-fluorenylmethoxycarbonyl) [17]. The peptide chain is constructed on an insoluble solid support, the resin, which enables the separation of the intermediate peptides from the

soluble reagents and solvents, by filtration. After the filtration of the resin from the soluble reagents, the intermediate peptide can be washed to prepare it for the next steps, the cleavage and the purification.

The C terminal amino acid of the target peptide is attached to the resin via the carboxyl group. The functional groups of each amino acid side chains are protected with permanent protecting groups which are called permanent because they are resistant to the basic reactions conditions involved during peptide chain assembly. Besides the permanent side chain protecting groups each amino acid is temporary protected before entering the coupling reaction with the resin (for the first amino acid attached on the C terminus) or with the next amino acid that couples. The Fmoc strategy is based on using two types of protecting groups:

a) The N-Fmoc group, which is the temporary protecting group and it can be removed under basic conditions and

b) The side chain permanent protecting groups and the linkage between the resin and the growing peptide chain, which are removable under acidic conditions.

In our synthesis of the beta amyloid peptide sequences the permanent protecting groups of the amino acids used were t-butyl and trityl, both of them being easily removable using TFA (trifluoroacetic acid, CF_3CO_2H).

The synthesis process is performed automatically and it follows three steps:

- N-Fmoc deprotection
- Activation of the carboxylic group of the amino acid
- Coupling step

The deprotection of the N-Fmoc group is done under basic conditions (20-50% v/v piperidine in DMF). In the first step the resin reacts with the first amino acid. If sites on the resin are not reacted in this loading process, they can be reacted during the next steps, generating C-terminus truncated by-products.

The resin used was a Rink resin (2-chlorotritylchloride resin) and it was chosen to give an amidated peptide, and because the coupling process is free from enantiomerization or dipeptide formation [17].

To test the resin deprotection before the first amino acid attachment, the ninhydirn (or Kaiser) test was used, following a standard protocol [26]. Several resin beads were removed from the reaction block and washed three times with ethanol. Then a mixture of ninhydrin (in EtOH)/ phenol (in EtOH)/ KCN (in piridine) in equal volumes was used to treat the beads. The solution is mixed well and heated at 120^0C for 4-6 minutes. If the color of the solution and the beads are dark blue, the deprotection was achieved, if not, the amino protecting groups are still attached to the resin and the coupling will not be efficient.

The coupling step in which the amide bond is formed involves the chemical activation of the carboxy component. Mild activating methods and reagents are preferred, mostly based on “in situ” generated active esters. In our synthesis we used as coupling reagents: HBTU (N-[(1H-benzotriazol-1-yl)(dimethylamino)methylene]-N-methylmethanaminium hexafluorophosphate N-oxide), HOBt (1-hydroxybenzotriazole) and DIPEA (diisopropyl ethylamine).

2.2.2 Post Synthesis Treatments of the Peptides

After the synthesis, the resulting peptide is still attached to the resin and each amino acid residue has the permanent protecting groups onto it. The permanent protecting groups attached to the amino acids are stable to the basic conditions during the peptide synthesis process, but they can be removed by cleavage under acidic conditions. Two other steps will follow:

a) The cleavage reaction

b) The purification of the crude peptide.

a) The cleavage reaction is performed under acidic conditions, which enable the removal of the permanent side chain protecting groups. Before starting the cleavage procedure, the resin should be dried for several hours on a lyophilizer to remove the water and volatile salts.

The cleavage reaction is done with TFA. Because of the cysteine presence in the sequences ethane dithiol was added to the cleavage cocktail. The role of ethane dithiol is to assist in the removal of the trityl protecting group from cysteine [33]. The typical cleavage cocktail is a mixture of TFA, ethane dithiol, distilled water and triisopropylsylane in a proportion of 94 /2.5 /2.5 /1 % v/v. This cocktail is poured onto the resin loaded with the peptide, and the resulted solution is stirred with a magnetic bar for several hours (2-4 hours). For the sequences synthesized, bamc16-20, bamc16-22, and bam16-22, the color of the resin beads changed right after adding the cleavage cocktail from pale yellow (the color of the dried resin beads) to red-pink, deep orange and deep yellow respectively. At the end of the cleavage reaction the beads had a similar color with their color before the synthesis (very pale yellow).

b) Purification of the crude peptide is necessary because the synthesis and the cleavage steps will yield a mixture of various peptides and byproducts beside the desired peptide. The purification is done by reverse phase liquid chromatography using an analytical column or a semiprep column, if larger amounts of peptides are purified. For purification of the peptides different methods were used. The methods were optimized to obtain a better resolution of the peaks and to afford a shorter elution time. For the analytical column the flow rate employed was 0.5 mL/min and 2 mL/min for the semiprep column.

The instruments used for peptide purification and study was a System Gold High Performance Liquid Chromatography (HPLC) System from Beckman Coulter, equipped with a 168 nm diode array detector and chromatographic software (32 Karat). The samples were delivered with a 200 μL injection loop.

The columns employed in our experiments were produced by Beckman-Coulter: analytical and semiprep, and both of them had the packing material composed of silica particles reacted with organochlorosilane which coats the particles surfaces with hydrocarbon chains that makes the particle surface hydrophobic. The particle diameter was 5 μm and the pores were 80 Å. The length of the columns was 250 mm, and the internal diameter was 4.6 mm for the analytical column, and 10 mm for the semiprep column.

Typical solvents were used for the RP-HPLC: water/acetonitrile. The composition of solvents was: A-99.9% HPLC grade water; 0.1% trifluoro acetic acid (Sigma Aldrich) and B-99.9% HPLC grade acetonitrile (Alfa Aesar) and 0.1% trifluoroacetic acid.

For purification of the peptides different methods were used. The methods were optimized to obtain a better resolution of the peaks and to afford a shorter elution time. The gradients varied between 2%ACN per minute and 4% ACN per minute, and after the peptide elution, the collected solution was frozen with liquid nitrogen and dried on the lyophilizer to be stored for further experiments.

The cysteine attachment in two of the peptides synthesized made necessary the use of a specific reagent to test its presence in the product, Ellman's reagent 5, 5'-dithiobis (2nitrobenzoic acid). The Ellman's reagent was purchased from Aldrich. A fresh solution of Ellman's reagent was prepared by dissolving 4 mg 5, 5'-dithiobis (2nitrobenzoic acid) in 1 ml phosphate buffer 0.1 M (pH 8.0). The peptide sample was dissolved in 200 μL phosphate buffer and 20 μL Ellman's reagent solution previously prepared was added. The mixture was allowed to react for 15 minutes at room temperature. The reaction between the peptide and the Ellman's reagent was monitored at 415 nm, checking the absorbance of the product on HPLC.

2.3 Experimental Section

2.3.1 Peptide Synthesis

The peptide synthesis was done with a Synergy Personal Peptide Synthesizer from Applied Biosystem. The amino acids and the resin were purchased from Nova Biochem and they were used as received. The solvents were purchased from Alfa Aesar and they were used as received. The amino acids are protected with permanent protecting groups and with temporary protecting groups (Fmoc).

The amounts of amino acids and of resin that were loaded into the empty columns were calculated with the formula provided by Synergy kit:

-The amino acids:

Derivative Molecular Weight (mg/mmol) X 0.075mmol = Derivative Weight (mg)

-The resin:

$$\frac{0.025mmol \times 1000}{resin\ substitution(mmol/g)} = \text{Resin Weight (mg)}$$

The resin used had a 0.059 mmol/g substitution and the maximum load was 0.03 mmol. The yields obtained varied between 60-70%.

For the synthesis we used for each amino acid entering the coupling reaction: 42.3 mg Rink resin, 43.90 mg cysteine (C) 35,14 mg lysine (K), 26.50 mg leucine (L), 25.45 mg valine (V), 29.05 mg phenylalanine (F), 23.34 mg alanine (A) and 31.9 mg glutamic acid (E).

2.3.2 Peptide cleavage

The cleavage reaction was performed using a standard TFA protocol. The reagents trifluoroacetic acid (TFA), triisopropylsilane (TIS) and ethanedithiol (EDT) were purchased from Aldrich and used as received. The cleavage cocktail is a mixture of TFA, ethane dithiol, distilled water and triisopropylsylane in a proportion of 94 /2.5 /2.5 /1 % v/v. We used 1880 μL TFA, 50 μL EDT, 50 μL distilled water and 20 μL TIS. This cocktail was poured onto the preweighed resin, stirred with a magnetic bar, and the vial was capped. The cleavage reaction was followed by the precipitation of the peptide with cold ether (6 mL) [33]. After the precipitation, the peptide was extracted with distilled water (6-8 mL). Then, the crude peptide was frozen with liquid nitrogen and dried overnight on a lyophilizer. After the freeze-dry process the products were obtained with yields varying between 30-60%, and were stored for future utilization.

2.3.3 Peptide purification

The dried peptides were suspended in distilled water and purified by HPLC Beckman-Coulter 168 nm detector using a semiprep column. For the purification of the crude peptide, each time 1mg dried peptide was dissolved in 1ml distilled water.

The purification method used for the beta -amyloid (bam16-22) sequence was: 3%ACN/ min, over 30 minutes with a flow rate of 2 mL/ min. The injection loop was 200 μL volume and the peptide load was 200 μg/ μL for each injection. For the peptide purification a semiprep column was used. The retention time was 27.5 min. The major peak was collected, frozen and lyophilized.

The purification method used for the beta-amyloid (bamc16-20) sequence was: 2%ACN/ min, over 30 minutes with a flow rate of 2 mL/ min. The injection loop was 200 μL volume and the peptide load was 200 μg/ μL for each injection. It was used a semiprep column. The retention time was 25.3 min. The major peak was collected, frozen and lyophilized.

For the beta amyloid sequence with cysteine in position 15, bamc16-22 the method was 4%ACN/ min, over 30 minutes, with a flow rate of 2 mL/min. The retention time was 21.0 min.

To check the cysteine presence in the sequences Ellman's reagent was used and the reaction with the thiol group was monitored by HPLC using the analytical column and a flow rate of 0.5 mL/min. The detection was performed at 215 nm and at 420 nm.

Chapter 3

Nanowires Assembly with Beta-amyloid Peptides

3.1 Gold Nanowires

One dimensional nano structures such as metal nanowires are expected to play an important role as building blocks for nano-assembled materials and devices. Their synthesis is difficult, mostly because at this scale it is complicated to control the morphology, the purity and the chemical composition. Nanowires are obtained through electrochemical deposition, using templates that allow obtaining nanowires with predetermined length and diameter. Some of the templates that have been used include biological macromolecules such as DNA strains or rod-shaped viruses [18].

The nanowires used in our experiments were obtained through electro-deposition and were synthesized in Dr. Wiley's lab (UNO, Department of Chemistry) by Ran Liu. To study the self assembly of the beta amyloid peptides (bamc16-20 and bam16-22) with nanowires, two types of nanowires were employed: pure gold nanowires (Figure 1), and symmetrical wires (Figure 2), composed by nickel and gold.

Figure 1 Gold nanowires

Figure 2 Symmetrical gold-nickel nanowires

The gold nanowires reactions with the peptides bamc16-20 and bam16-22 were monitored using HPLC techniques.

3.2 Studying the Interactions between Beta-amyloid Short Sequences Peptides and Gold Nanowires – Experimental Design

In order to test our hypothesis that bio-systems can be self-assembled with gold nanowires we designed our experiments to follow the chart-flow presented in Figure 3.

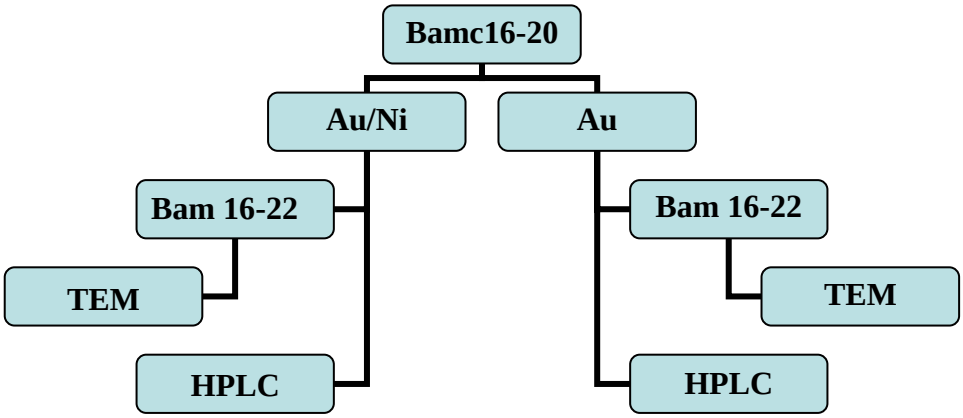

Figure 3 Experimental design for studying the self-assembly of gold nanowires with the peptides bamc16-20 and bam16-22

We studied using HPLC, the aggregation of bamc16-20 peptide as a function of time to have a control experiment. We monitored the adsorption process of the peptide bamc16-20 onto the nanowires by HPLC using an analytical column and a 0.5 mL /minute flow rate. Then, the wires with the bamc16-20 peptide were treated with the fibril forming peptide bam16-22 (KLVFF) and the result was studied with the TEM.

From the two types of wires (stored in methanol) 50 μL wires containing solution was taken and transferred into separated eppendorfs, combined with 50 μL distilled water, then frozen and lyophilized, to obtain the wires only. To the 4 eppendorfs

containing the wires (which are magnetically active) was added a solution of the bamc 16-20 sequence. The solution was obtained diluting the peptide samples purified (one at the time) with 50 μL distilled water. After this step the 4 eppendorfs containing the wires and the peptide bamc16-20 solution were sonicated for 30 seconds. After the sonication step, the wires with the peptide adsorbed onto them were separated from the peptide bamc16-20 solution with the help of a magnet. The solution of the peptide was pipetted out of the eppendorfs, and the wires with the peptide adsorbed onto them are found at the bottom of the eppendorfs. The bam 16-22 (the fibril forming peptide) was added to the wires and the resulted product was analyzed in a time-course experiment with the TEM.

Transmission electron micrographs (TEM) and electron diffraction patterns were obtained using a JEOL 2010 TEM operating at 120 V. The samples were prepared by mounting small aliquots of the peptides/wires solution on TEM copper grid and dried overnight, then, directly loaded in TEM for observation.

3.3 Characterization of Beta-amyloid Short Sequences Peptides Interaction with Gold Nanowires Using HPLC Techniques

The aggregation of beta amyloid peptides bamc16-20 was monitored with HPLC in the absence of the gold nanowires as a control experiment and the result is presented in Figure 4. It can be seen that the aggregation process occurred in less than five hours. The peak area from each chromatogram performed was measured and the result was plotted as a function of time.

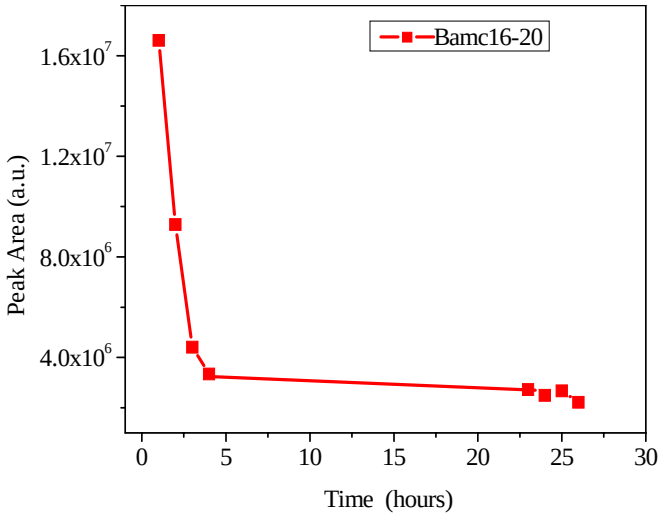

Figure 4 Aggregation of bamc16-20 monitored for 26 hours.

The adsorption of the bamc16-20 peptide onto the gold/nickel nanowires was observed by HPLC and the results are presented in Figure 5. The peak area was measured for each chromatogram performed during a 26 hours time period and the results were plotted as a function of time. To compare the aggregation of the peptide bamc16-20 in the presence of Au/Ni nanowires and the aggregation of the peptide by itself, the results for these two experiments were plotted as a function of time on the same graph (Figure 5).

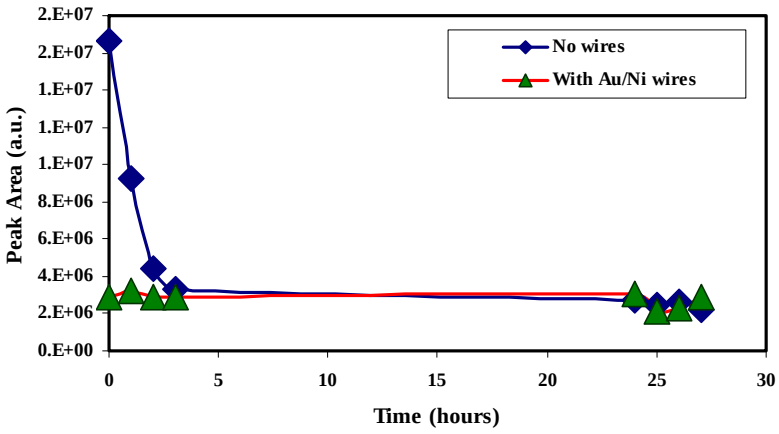

Figure 5 Comparison of aggregation rate of bamc16-20 by itself and with the Au/Ni nanowires.

To compare the results of the time-course experiments with the gold nanowires and gold/nickel nanowires, we plotted on the same graph the peak area for each chromatogram and the results are presented in Figure 6.

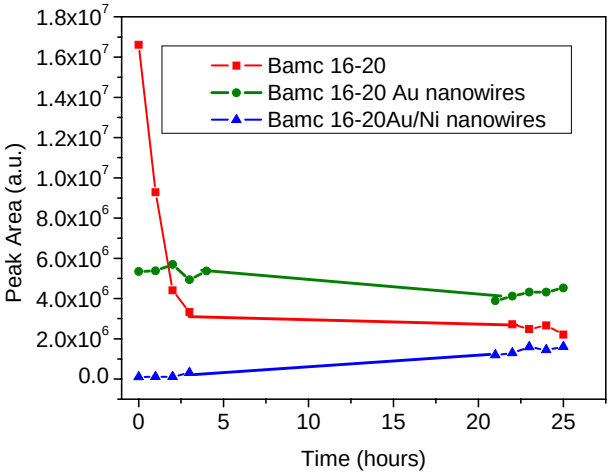

Figure 6 Comparison for bamc16-20 aggregation in time in presence of the nanowires

The reproducibility of the experiments performed to study the self-assemble of the two types of nanowires used was checked several times, and the results of these experiments are presented in Figure 7. For each time-course experiment performed, the area of the peak resulted from the chromatogram was plotted as a function of time

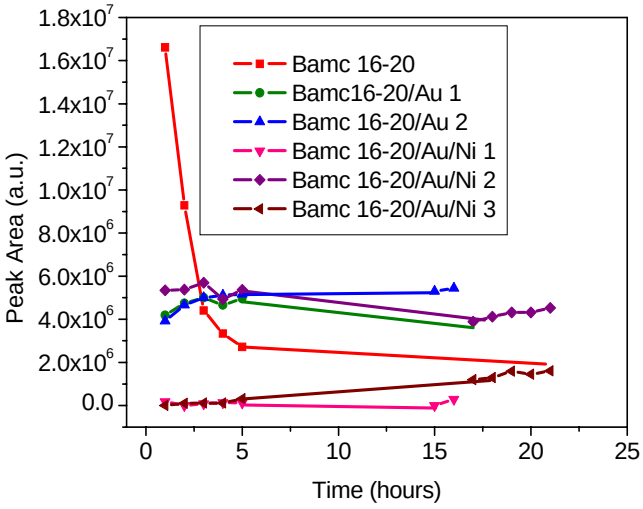

Figure 7 Comparison of the results for time-course experiments for the aggregation of bamc16-20 peptide in the presence of gold nanowires.

The results obtained from the time-course experiments performed using HPLC suggested that the aggregation of bamc16-20 peptide in the presence of the gold nanowires occurs very fast, and the use of HPLC to analyze the aggregation process is inefficient for this study.

3.4 Characterization of Beta-amyloid Short Sequences Peptides Interaction with Gold Nanowires Using TEM

The TEM images were taken from the samples of bamc16-20 adsorbed onto the gold nanowires and Au/Ni nanowires, which were then treated with bam16-22 fibril forming peptide. The images revealed the formation of fibrils with different shapes, and different dimensions. The nanowires were not observed in these samples. The nanowires used had dimensions of 5 μm and there is the possibility that during the sonication step they were broken in smaller pieces. In Figure 8 the magnification used was 25 K and the fibril has a length of 3 μm and a width of 0.6 μm. We believe the darker spots that can be seen inside are, probably, fragments of the nanowires which were coated with the peptide. In Figure 9, Figure 10, Figure 11 and Figure 12 are images of the peptides fibrils formed by aggregation with the fragments of the nanowires.

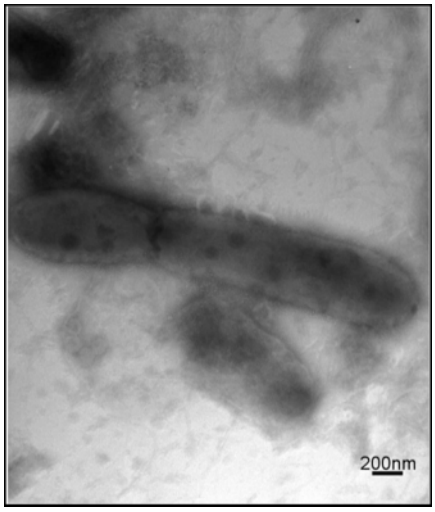

Figure 8 Fibrils of bamc16-20 /bam16-22 aggregated in the presence of gold nanowires

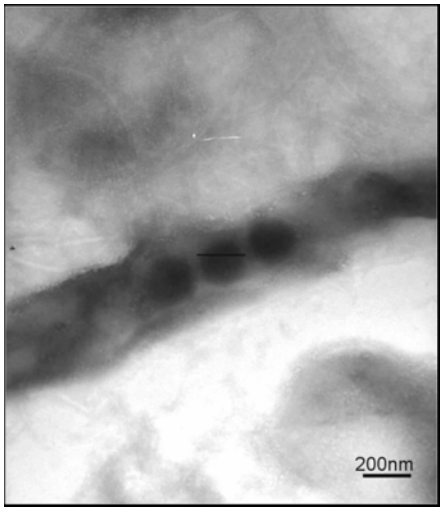

Figure 9 Fibrils of bamc16-20 /bam16-22 aggregated in the presence of gold nanowires

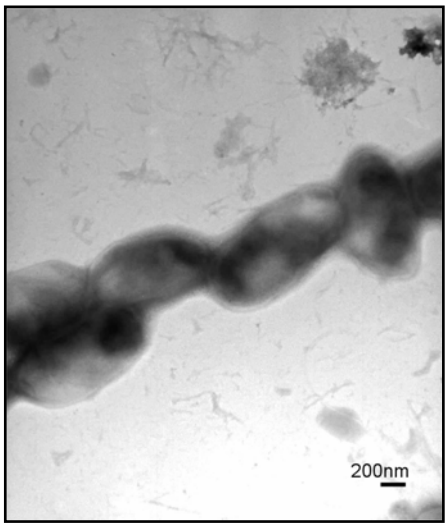

Figure 10 Fibrils of bamc16-20 /bam16-22 aggregated in the presence of gold nanowires

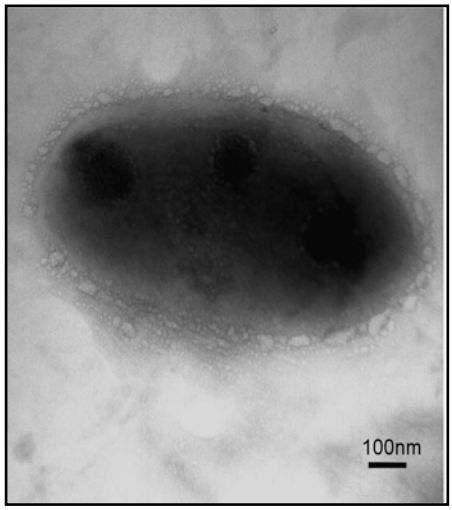

Figure 11 Fibrils of bamc16-20 /bam16-22 aggregated in the presence of gold nanowires

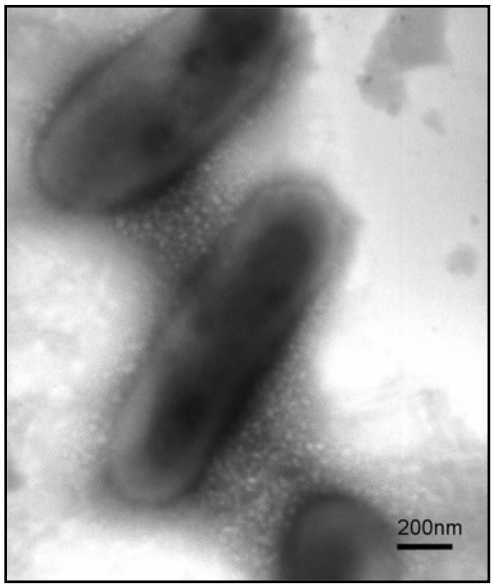

Figure 12 Fibrils of bamc16-20 /bam16-22

aggregated in the presence of gold nanowires

3.5 Conclusions

Gold nanowires were treated with the peptide bamc16-20 and bam16-22, and the assembling process was monitored using HPLC techniques and TEM. The experiment was not reproducible, probably due to the fact that the nanowires were broken during the lyophilization or the sonication steps. The nanowires used to be self-assembled with the beta-amyloid short sequences peptides were about 5 μm length and they were much larger than the peptides. The difference in the scales of the nanowires and the peptides lead us to the idea to self-assemble the short sequence of beta-amyloid peptide with smaller nano-materials.

Chapter 4

Gold Nanoparticles Self-assembly with Beta-amyloid Short Sequence Peptide

4.1 Introduction

Colloidal gold is well known for several hundred years [20], but their use as investigational solution has emerged only in the last century when their synthesis methods were improved, which allowed a better understanding of the colloidal processes in general. Colloids are stable dispersion of a phase (solid- Au particles) in another (liquid- the solution in which the gold particles are suspended). The composition of colloidal gold particles consists of an elemental gold core surrounded by a double layer of charges: a negative inner layer ($AuCl^-_2$ ions adsorbed on the surface of the crystalline gold core) and a positive outer layer (H^+ ions).

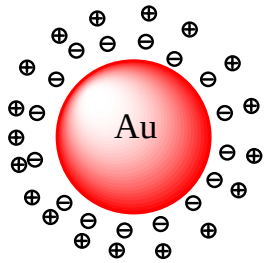

Figure 13 Double layers of charges surrounding the gold particle in colloidal solutions.

The surface layer surrounding the gold crystalline core is responsible for the negative charge of the colloidal gold and its stability with respect to aggregation. The negative charge layer arising from the residual negative ions in solution is called the zeta potential and provides the means for the gold particles to repel one another and to stay in suspension indefinitely [20].

Gold colloids are synthesized using various methods to obtain particles with diameters ranging on a scale from 0.5 nm to 60-80 nm [21]. In most of the synthetic methods, the tetrachloroauric acid is reduced under various conditions. The reducing agents can be: thiocyanate (NaSCN), white phosphorus, borohydride or sodium citrate and tannic acid. The dimensions of the gold nanoparticles that result depend on the type of the reducing agent used. When the reducing agent is added, the gold ions in solution are oxidized from the ionic form to gold atoms. As the reducer is added a rise in gold atom content in the solution appears until a saturation level is reached, followed by a supersaturation. Aggregation then occurs, in a process called nucleation, to form central icosahedral gold cores of 11 atoms at nucleation sites. The formation of nucleation sites, in order to reduce the supersaturation of gold atoms in solution, occurs extremely quickly. After the saturation level is achieved, the remaining gold atoms in solution continue to bind to the nucleation sites until all atoms are removed from solution (supersaturation).

The number of nuclei formed initially determines how many particles finally grow in the solution. This number, in turn, depends on the amount of reducing agent added. A large amount of reducer produces a large number of nucleation sites and so, a large number of gold particles are produced. The larger the number of nucleation sites for a given amount of gold chloride in solution, the smaller will be the final size of each gold particle. Particle size can be carefully controlled by the amount of reducer added. If the manufacturing conditions are optimized, the nucleation sites will be formed instantaneously and simultaneously, and all gold particles will grow to exactly the same size. This is a very difficult task to accomplish and, most manufacturing methods can not

achieve instantaneous reduction and formation of nucleation sites, resulting in uneven growth of the colloidal gold particles. The interaction of gold nanoparticles with proteins or peptides is achieved by bonding formed between the sulfur atoms (thiol groups) present in the peptides and the gold atoms [25].

4.2 Gold Nanoparticles Characterization using TEM and UV-Vis Spectroscopy

The gold nanoparticles used in our experiments were purchased from Sigma. The use of uneven gold nano particles can cause irreproducible results and unstable conjugates. Transmission electron microscopy examination is the only true way to determine the quality of colloid, to determine whether a colloid or conjugate contains fused, aggregated, or heterogeneous particles, or a mixed-size population. The TEM images of the gold nanoparticles (GNP) 5 nm and gold nanoparticles (GNP) 10 nm were taken to analyze the colloidal solutions before using them in experiments. In Figure 14 and Figure 15 are presented TEM images of gold nanoparticles of 5 nm and 10 nm respectively, and it can be seen that the nanoparticles are relatively homogeneous with respect to their size and shape, and are not aggregated.

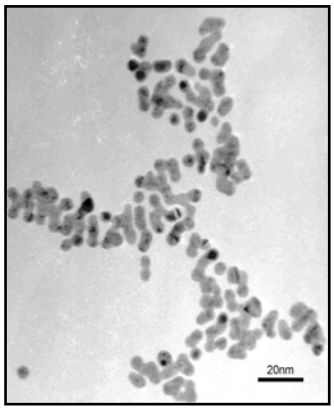

Figure 14 TEM image of GNP 5 nm.

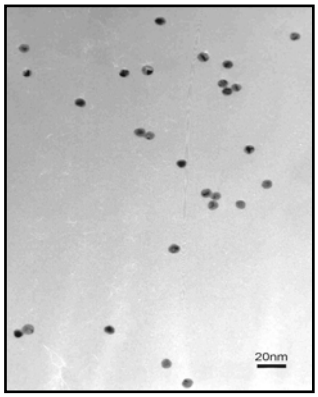

Figure 15 TEM image of GNP 10 nm.

The UV-Vis spectrophotometrical measurements performed to establish the wavelength at which the maximum absorbance occurs were done by scanning the wavelength between 300 nm and 900 nm. For the 5 nm gold nanoparticles the wavelength was found at 517 nm. For the 10 nm gold nanoparticles, the wavelength at which the maximum absorbance occurred was found at 521.6 nm. The values obtained for the wavelength corresponding to the maximum absorption (λ_{max}) are in agreement with values reported for similar gold nanoparticles sizes, smaller values of λ_{max} corresponding to smaller sizes of the gold nanoparticles [22].

4.3 Experimental Design to Study the Self-assemble of Gold Nanoparticles with Beta-amyloid Short Sequence Bamc16-22

To study the self-assemble of the gold nanoparticles with bamc16-22 peptide we used UV-vis absorption spectroscopy and TEM.

The experiments performed for the study of the self-assemble of the gold nanoparticles 5 nm are schematically shown in Figure 16. PHSB stands for phosphate saline buffer and CR for Congo Red.

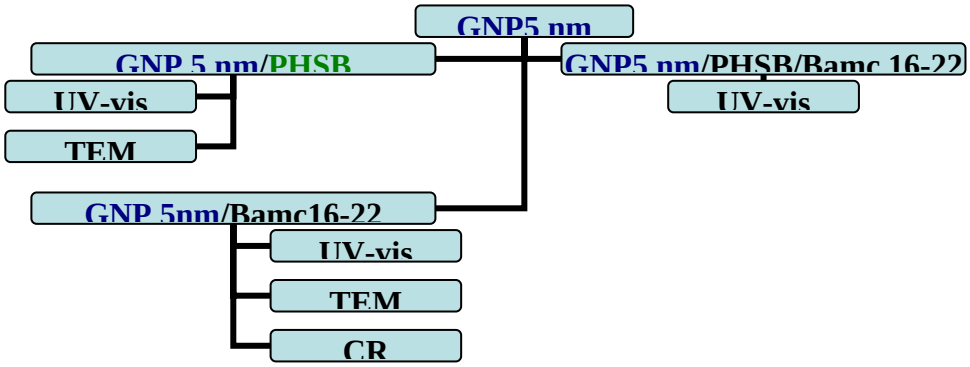

Figure 16 Experimental design to study the self-assemble of 5 nm gold nanoparticles (GNP 5 nm).

For the 10 nm gold nanoparticles the same experiments were performed and they are schematically shown in Figure 17.

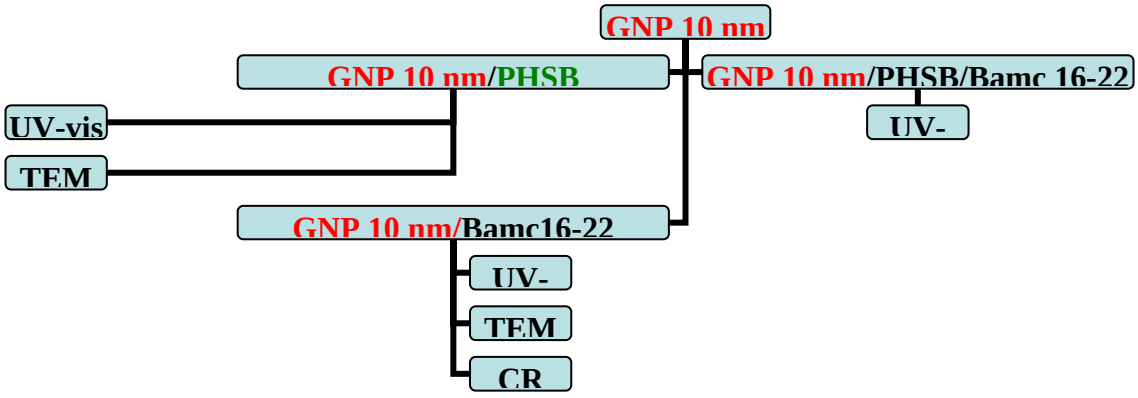

Figure 17 Experimental design to study the self-assemble of 10 nm gold nanoparticles (GNP 10 nm).

We checked the behavior of the gold nanoparticles when diluted in 1:1, 1:10, 1:100 and 1:1000 proportions with phosphate buffer with a physiological pH (7.4), and the orange color of the colloidal solution changed to light blue, a sign that aggregation of gold particles occurred. The change in the color of the gold colloids was also monitored with spectrophotometrical techniques for various dilutions. The results from the UV-Vis measurements are presented in Table 1 for the 5 nm diameter gold nanoparticles. It can be observed from the UV-vis data that for the 5 nm gold nanoparticles a large red shift occurred when the phosphate buffer was added. The shift was observed for each of the dilutions scanned, but the larger shift was measured for the 1:1 volume dilution of the colloidal solution with phosphate buffer.

Gold Nanoparticles 5nm	**GNP5nm**	**GNP5nm/PHSB** (1:1)dilution	**GNP5nm/PHSB** (1:10) dilution	**GNP5nm/PHSB** (1:100)dilution	**GNP5nm/PHSB** (1:1000)dilution
λmax (nm)	517.0	632.0	558.6	312.4	308.2
Absorbance (a.u.)	0.763	0.307	0.085	0.026	0.023

Table1 Dependence of the maximum wavelength on the dilution with phosphate saline buffer (PHSB) for the 5 nm diameter gold nanoparticles (GNP 5 nm)

In the Table 2 are presented the results for the spectrophotometrical measurements performed for the10 nm diameter gold nanoparticles colloidal solutions diluted with phosphate saline buffer in various proportions.

Gold Nanoparticles 10nm	**GNP10nm**	**GNP10nm/PHSB** (1:1) dilution	**GNP10nm/PHSB** (1:10) dilution	**GNP10nm/PHSB** (1:100) dilution	**GNP10nm/PHSB** (1:1000) dilution
λmax (nm)	521.6	637.6	566.4	556.8	556.8
Absorbance (a.u.)	0.691	0.194	0.070	0.028	0.021

Table 2 Dependence of the maximum wavelength on the dilution with phosphate saline buffer (PHSB) for the 10 nm diameter gold nanoparticles (GNP10 nm)

The shift measured for the 10 nm gold nanoparticles was larger than the shift observed for the 5 nm gold nanoparticles, suggesting that the aggregation was greater for the 10 nm particles than for the 5 nm particles.

Images taken with TEM of the gold nanoparticles of 5 nm and 10 nm diameters after adding the phosphate saline buffer (PHSB) are presented in Figure 18 and Figure 19. In both cases, the aggregation results obtained from the UV-Vis measurements for the gold nanoparticles were verified.

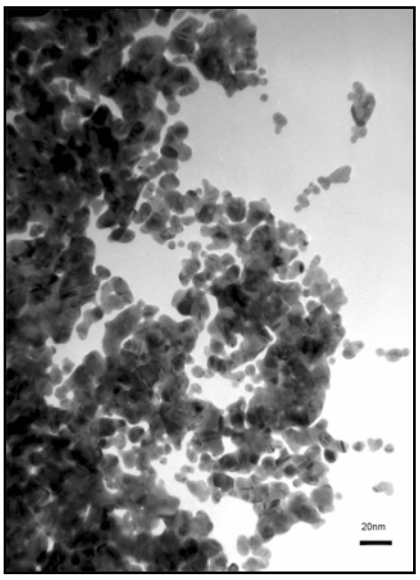

Figure 18 TEM image of GNP 5 nm aggregated in PHSB

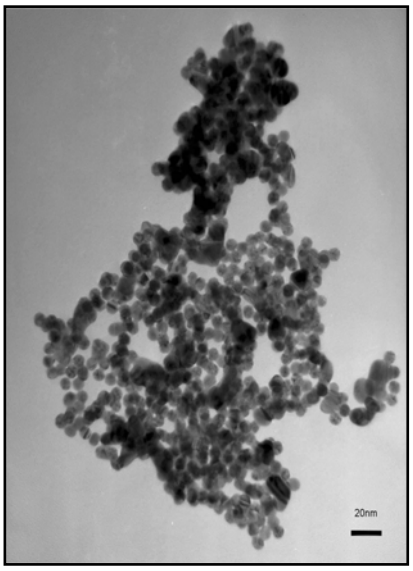

Figure 19 TEM image of GNP 10 nm aggregated in PHSB

4.4 Studying Self-assembly of Beta-amyloid Bamc16-22 Peptide with Gold Nanoparticles Using UV-Vis Spectroscopy

The colloids were diluted with phosphate saline buffer prepared in our lab (pH 7.4) to check their behavior at a physiological pH.

The peptide bamc16-22 (0.2 mg) was dissolved in the colloidal solutions GNP 5 (300 μL) or GNP 10 (300 μL) and the reaction was monitored by measuring the absorbance of the mixture periodically for 168 hours. The samples were then mounted on copper grids and studied by TEM.

The gold colloids used were stable for the duration of the experiments and their stability was checked spectrophotometrically. After adding the phosphate buffer their color changed and a blue color and a deposit on the bottom of the eppendorf tubes was noticed, a sign that the aggregation of the particles occurred. The solutions of gold

nanoparticles 5nm (GNP5) and 10 nm (GNP10) mixed in proportion of 1:1 with phosphate buffer (v/v) were then monitored by UV-Vis. The results presented in Table 1 and 2 showed an increase in the maximum wavelength observed for the colloidal solution from 517 nm for GNP5 to 632 nm for the 1:1 GNP5/phosphate buffer mixture and from 521.6 nm for GNP10 to 637.6 nm for the 1:1 GNP10/phosphate buffer mixture.

Three kinetic experiments were performed in order to observe the rate of gold deposition. The absorbance was monitored for a period of 16 hours and the results obtained from these kinetic experiments are shown below in Figure 20.

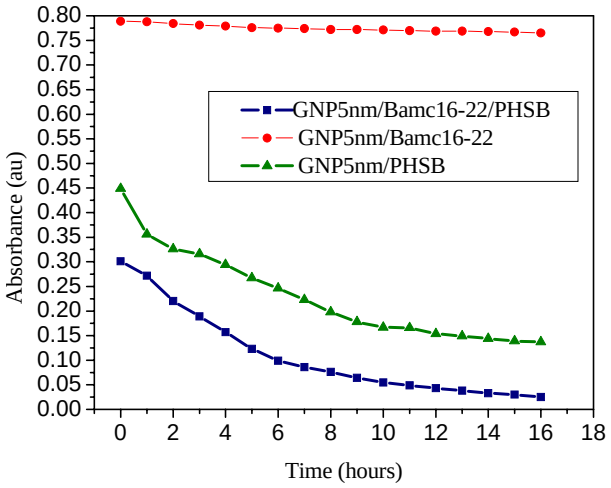

Figure 20 Deposition of GNP 5 nm in presence of bamc16-22 and/or PHSB

In the first experiment the 5 nm gold nanoparticles reacted only with the bamc16-22 peptide (red curve). Through the course of the second experiment they were treated with the phosphate buffer (green curve), and in the third one the 5nm gold nanoparticles were treated with bamc16-22 dissolved in phosphate buffer (black curve). In second and third experiments, where the 5 nm gold nanoparticles were mixed with the phosphate buffer, the aggregation was fastest during the first 7 hours. Comparing the three curves in Figure 20 it can be seen that the aggregation process was slower for the solution

containing only the peptide and the gold nanoparticles, as opposed with the solutions containing the buffer or the buffer/ bamc16-22 mixture.

In Figure 21 is presented a comparison between the behaviors of 10 nm gold nanoparticles when treated only with the beta amyloid peptide (red curve), with the phosphate buffer (green curve) and with the peptide dissolved in the phosphate buffer (blue curve).

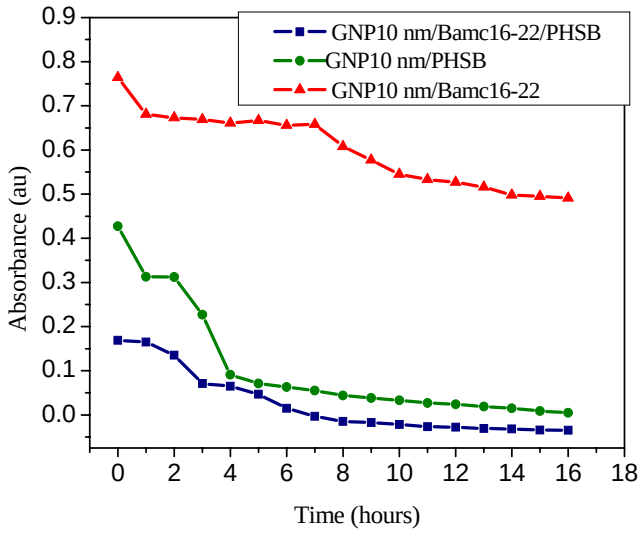

Figure 21 Deposition of GNP 10 nm in presence of bamc16-22 and/or PHSB

The results for the kinetic experiments for the 10 nm gold nanoparticles suggest that the process was slower for the solution containing only the peptide. The existence of the two inflexions points in the case of GNP 10 nm /bamc16-22 solution suggests that the process has 2 steps: the first one, the aggregation of the gold nanoparticles with the peptide, and the second one, the settling of the aggregates from the solution.

To compare the behavior of the two sizes of gold nanoparticles, 0.2 mg peptide bamc16-22 was mixed with 300 μL GNP 5 nm or GNP 10 nm colloidal solutions. The

two solutions were scanned for 100 hours and the wavelengths corresponding to the maximum absorbances observed were plotted as a function of time. The results are presented in Figure 22.

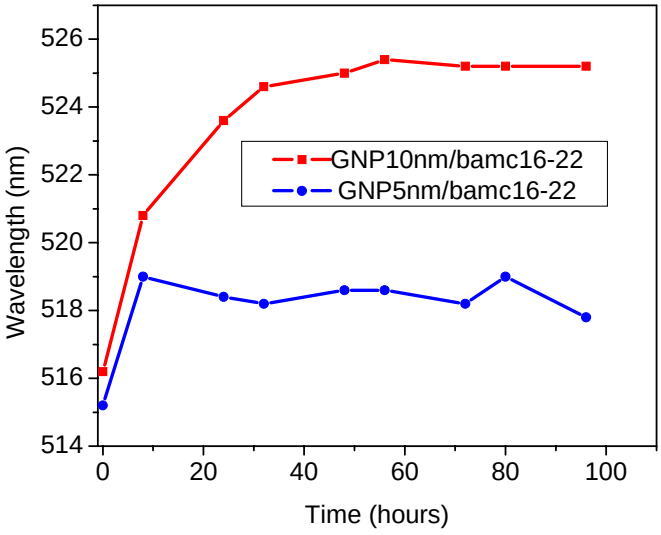

Figure 22 Comparison of the wavelength variation for the deposition process of the bamc16-22 peptide and gold nanoparticles of 5 nm and 10 nm.

The results for this experiment show that the increase in the wavelength values was larger for the 10 nm gold nanoparticles than for the 5 nm gold nanoparticles. The variation in the wavelength observed also suggests that the deposition process was complete after 10 hours for the 5 nm nanoparticles. For the 10 nm nanoparticles the increase in the wavelength value stopped after about 60 hours. The larger shift in the maximum wavelength observed for the 10 nm particles suggests a larger ability of this particles to react with the peptide bamc16-22 than the 5 nm gold nanoparticles. The longer reaction time for the 10 nm gold nanoparticles could be an indication that they form larger aggregates.

To study the structure of the gold nanoparticles assembled with the fibril forming peptide bamc16-22, samples of the peptide dissolved in the colloidal solutions were deposited onto copper grids and were dried overnight and observed with the TEM.

4.5 Studying Self-assembly of Beta-amyloid 16-22 Peptide with Gold Nanoparticles Using Transmission Electron Microscopy

The solutions for the TEM studies were obtained dissolving 0.2 mg bamc16-22 in 300 μL gold nanoparticles solutions of 5 nm or 10 nm. The solutions were vortexed for 30 seconds after the addition of the gold nanoparticles and kept at room temperature for seven days. After seven days, the solutions were mounted on the copper grids and dried overnight. The next figures represent the 5 nm gold nanoparticles reacted with the bamc16-22 peptide, and they are taken at various magnifications, at a voltage of 120V.

Figure 23a presents an image of the 5 nm gold nanoparticles (the black dots) reacted with the peptide. We supposed that the bead-like arrangement of the gold nanoparticles occurs as a result of the reaction with the peptide because the TEM images obtained for the gold nanoparticles by themselves show a different ordering manner (Figure 23b).

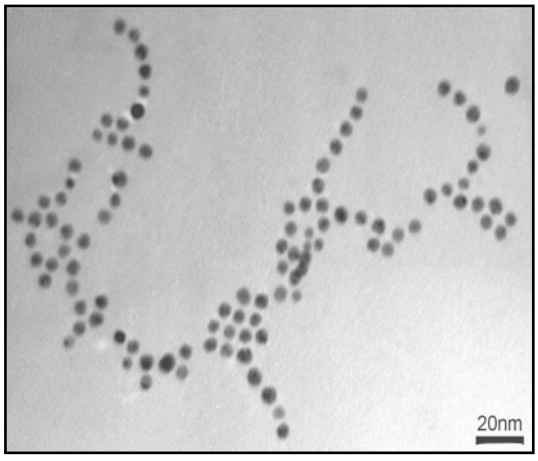

Figure 23a GNP 5 nm/bamc16-22

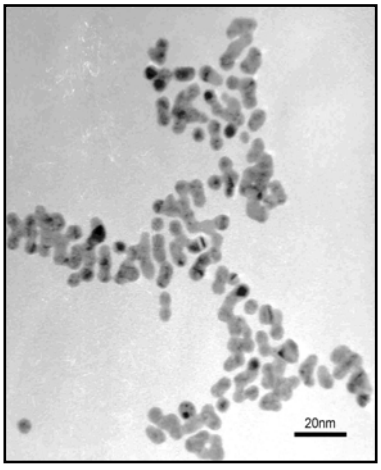

Figure 23b TEM image of GNP 5 nm

In Figures 24 a)-c) 5 nm gold nanoparticles are assembled with the peptide. We believe the darker gray shape is the peptide sheet. It can be observed that the gold nanoparticles reside mostly on the outer edge of the sheet, only few of them can be found on the peptide sheet. In Figure 24d) only four particles are assembled with the peptide.

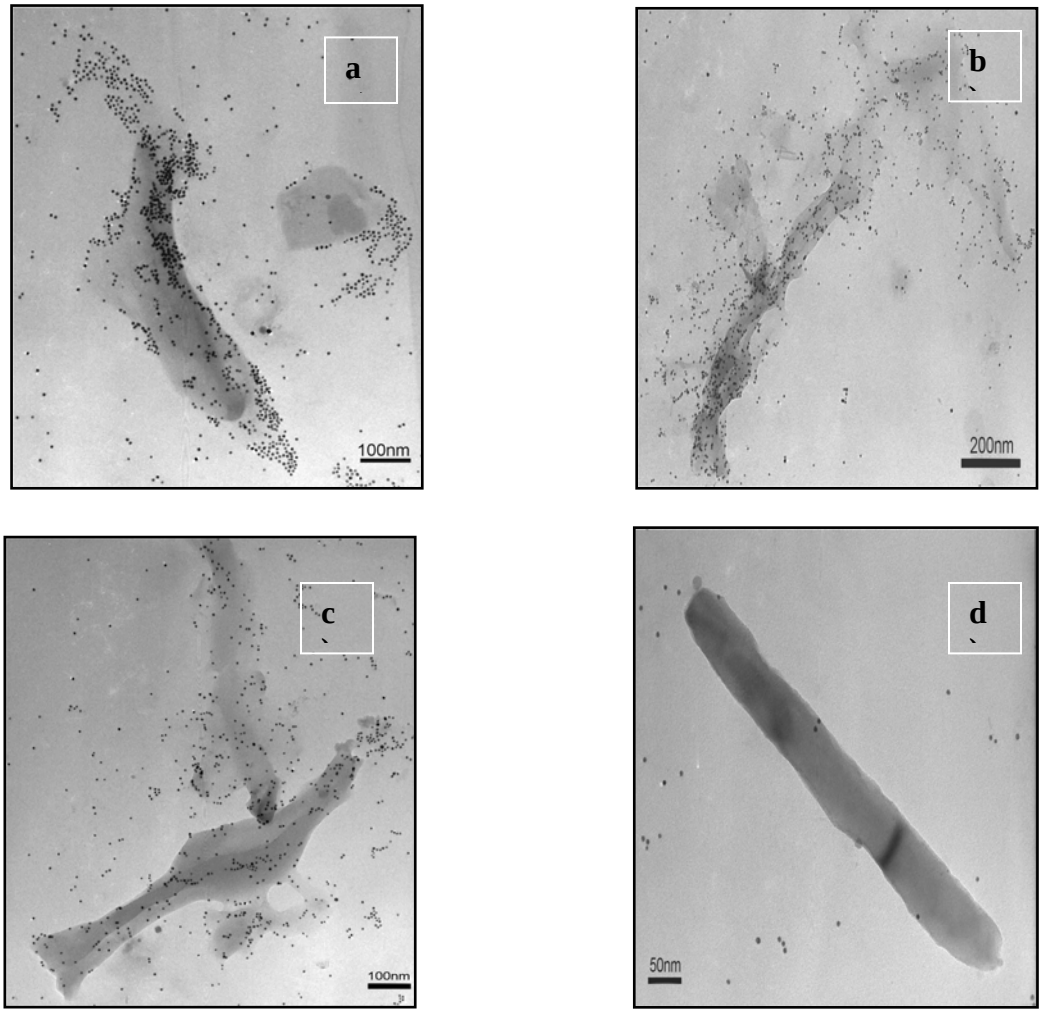

Figure 24 (a-d) GNP 5 nm attached to the bamc16-22 peptide beta sheets

The TEM images of the 5 nm gold nanoparticles seem to agree with the UV-Vis measurements previously performed. The smaller shift in the wavelength observed for the 5 nm gold nanoparticles was an indication that the 5 nm gold nanoparticles did not react

in a very large extent with the bamc16-22, as compared to the 10 nm gold nanoparticles for which a larger shift in the wavelength was measured.

The next figures represent TEM images of the 10 nm gold nanoparticles assembled with the bamc16-22 peptide, taken at various magnifications. Figure 25 a) and b) represents 10 nm gold nanoparticles ordered as beads.

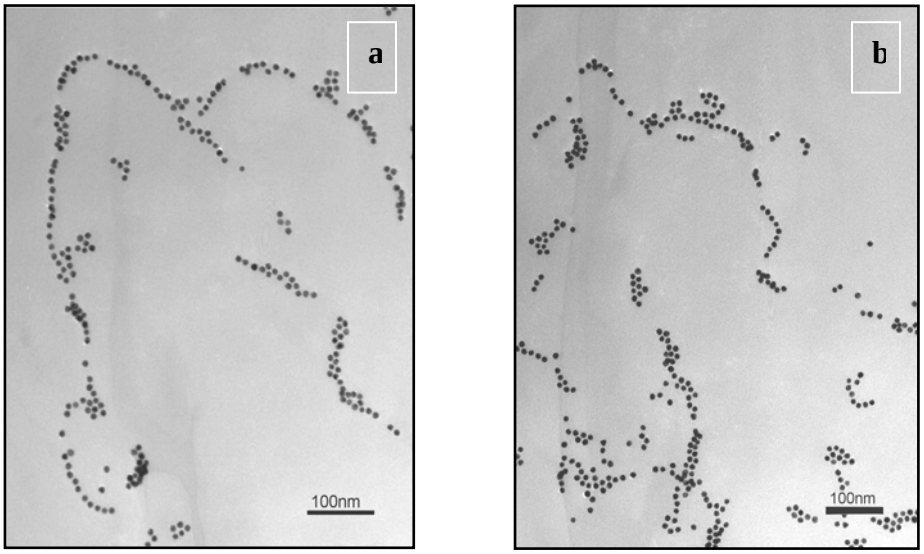

Figure 25 (a and b) GNP10 nm/bamc16-22, ordered as beads

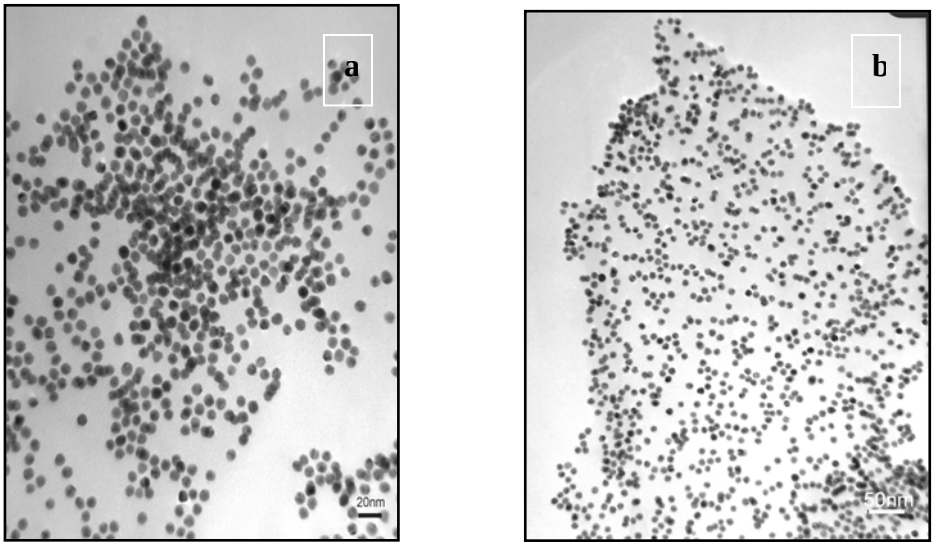

Figure 26 (a and b), GNP10 nm/bamc16-22 assembled as sheets

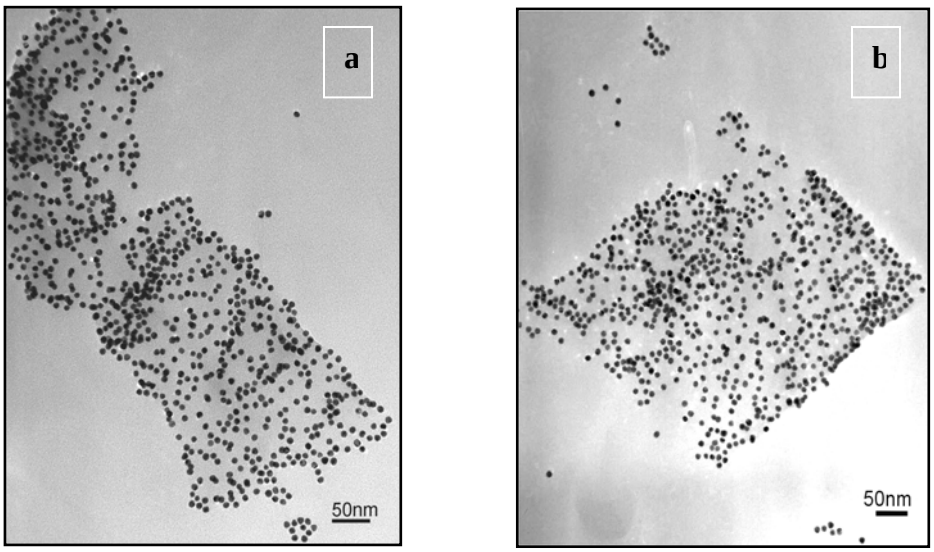

Figure 27 (a and b), GNP10 nm/bamc16-22 showing a ribbon-like assembly

The TEM images presented in Figures 26 and 27 show beta-sheets assembled with the 10 nm gold nanoparticles. It can be seen from them, that assemblies have very distinct edges and almost all the 10 nm gold nanoparticles seem to be assembled.

The Figure 28 represent a TEM image of a structure formed by the peptide beta-sheet assembled with the 10 nm gold nanoparticles.

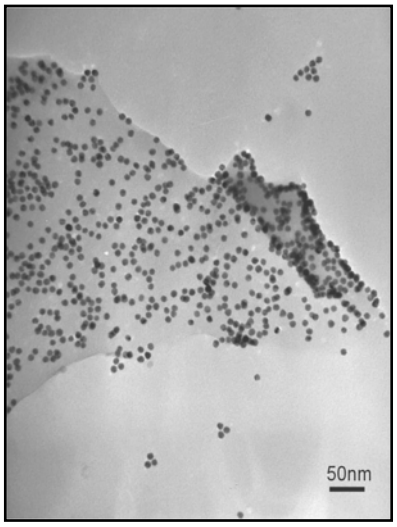

Figure 28 Bamc16-22 self-assembled with GNP 10 nm

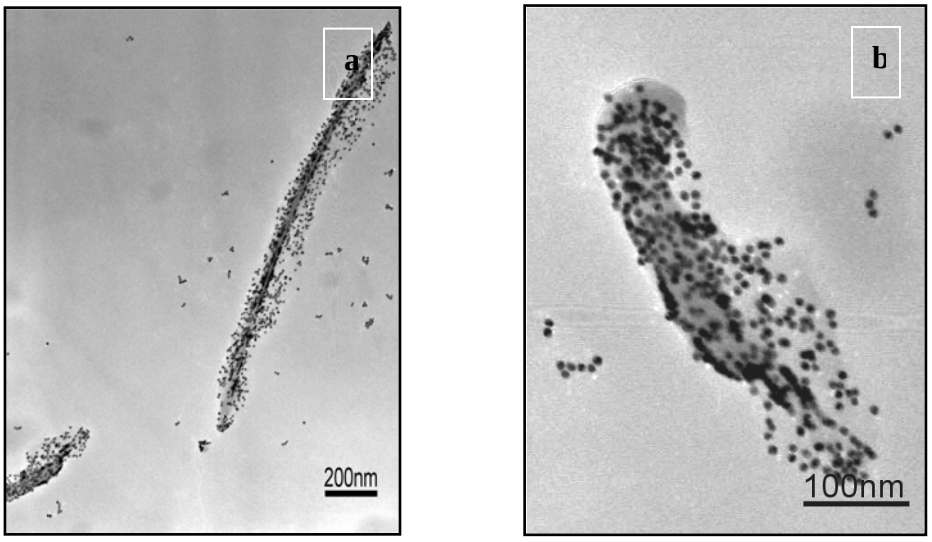

Figure 29 (a and b), GNP10 nm/bamc16-22 fibrils

The TEM images from Figure 29 a, b show fibrils formed from peptide bamc16-22 beta-sheets self-assembled with the 10 nm gold nanoparticles. Comparing the TEM images acquired from the self-assemble of the 5 nm gold nanoparticles with the images taken for the 10 nm gold nanoparticles, it can be seen that the 10 nm gold nanoparticles self-assembled in a larger extent with the peptide than the 5 nm gold nanoparticles. The result was in agreement with the UV-Vis spectrophotometrical measurements performed previously, where we observed a larger red shift in the maximum wavelength measured for the 10 nm gold nanoparticles than the one measured for the 5 nm gold nanoparticles. The various structures (sheets, ribbons and fibrils) observed are in agreement with the literature [7, 12, 19]. The presence of the beta-sheet in the fibrils formed by self assembling the bamc16-22 peptide with the gold nano particles was checked using Optical Light Microscopy on the samples stained with Congo Red.

4.6 Studying the Presence of Beta-sheets in Beta-amyloid Bamc16-22 Peptide Fibrils Using Optical Light Microscopy

We observed the fibrils formed by beta amyloid short sequence bamc16-22 peptide using an optical microscope Olympus BX 60M and Congo red staining [22-24]. The first sample was prepared by dissolving 0.2 mg peptide bamc16-22 in 300 μL distilled water. The solution was kept at room temperature for 7 days, and then 10 μL solution of Congo red was added to 50 μL bamc16-22 sample. The Congo red solution was obtained from Aldrich and used as received. In Figures 30 a-f are presented images of the peptide bamc16-22 stained with Congo red, taken with the optical light microscope under polarized light. The images reveal similarities with the TEM images previously obtained in our experiments, with respect to the shape of the fibrils, as expected.

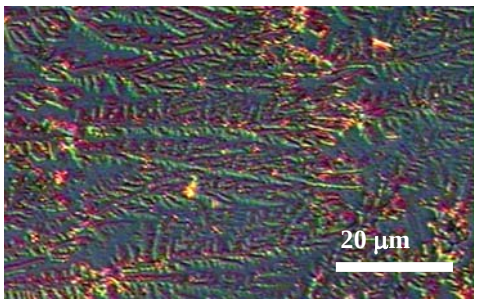

a)

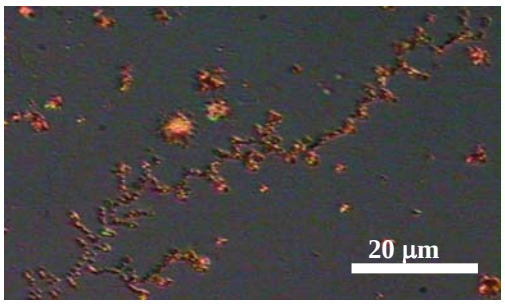

b)

c)

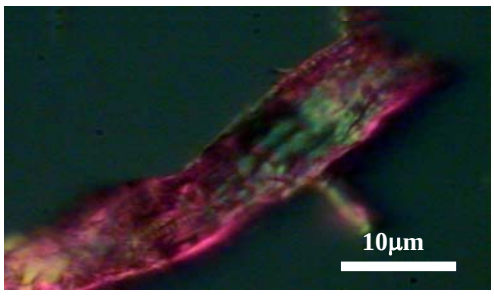

d)

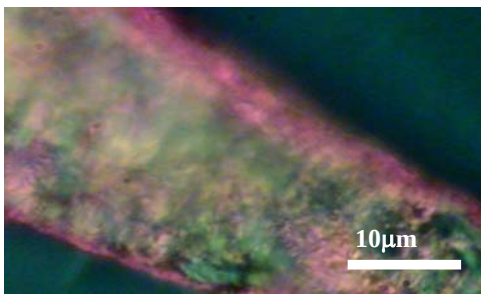

e)

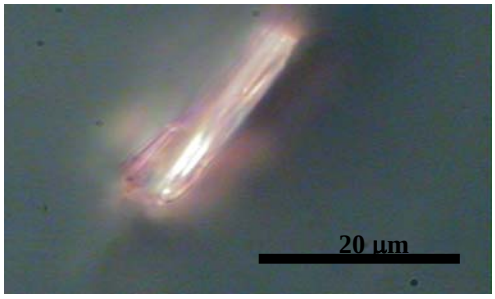

f)

Figure 30 a) - f) Beta amyloid 16-22 fibrils stained with Congo red and visualized by optical light microscope under polarized light.

Two samples of the peptide bamc16-22 assembled with the 5 nm gold nanoparticles and the 10 nm ones were prepared by dissolving 0.2 mg bamc16-22 in 300 µL colloidal solutions. After 7 days, the samples were stained by adding 10 µL Congo red solution to 50 µL solution of bamc16-22 and gold nanoparticles and visualized with the optical light microscope under polarized light in bright or in dark field. In Figure 28 a-c are presented images taken from the samples of the peptide combined with the 5 nm gold nanoparticles in dark field, and a'-c' represent the same images taken in bright field.

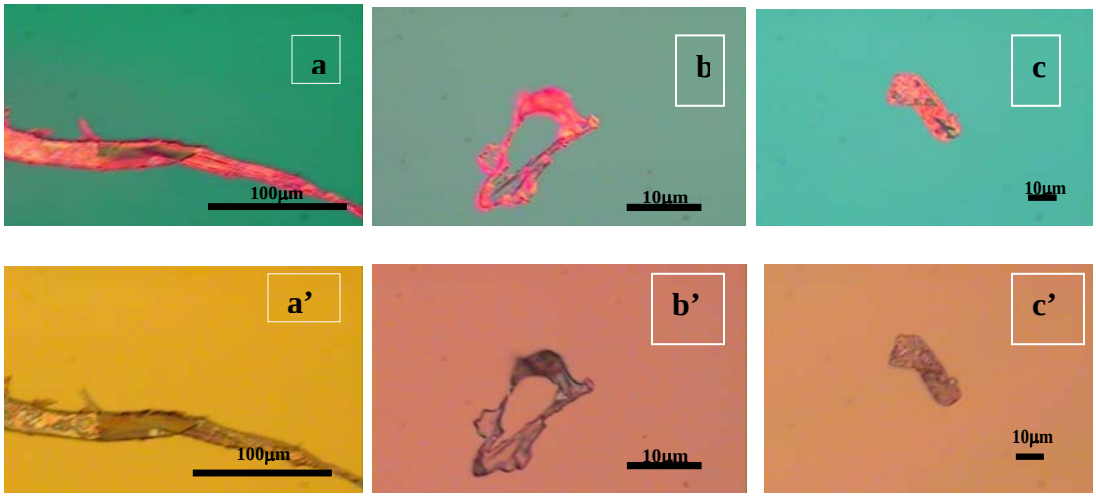

Figure 30 Fibrils of bamc16-22 combined with GNP 5 nm and stained with Congo red taken under polarized light in dark field (a-c), and in bright field (a'-c').

In Figure 31 are presented images of the peptide fibrils obtained by combining the peptide with the 10 nm gold nanoparticles. The images a-c were taken under polarized light in dark field, and the images a'-c' were taken in bright field.

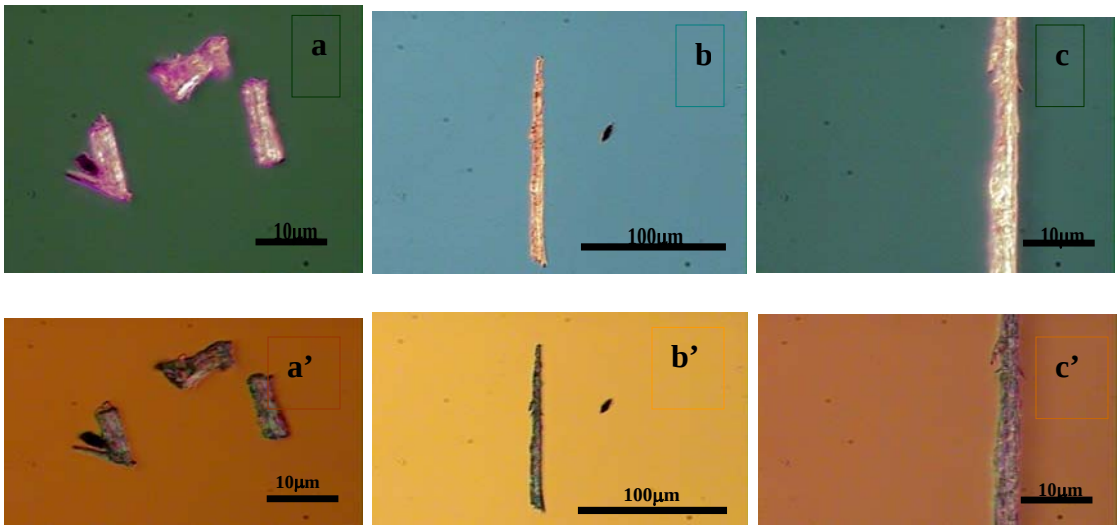

Figure 31 Fibrils of bamc16-22 combined with GNP 10 nm and stained with Congo red taken in dark field (a-c) and in bright field (a'-c').

In all the cases the yellow-green birefringence specific to the beta-sheet presence was observed. The fibrils observed by optical light microscope resemble with the fibrils observed by transmission electron microscope.

4.7 Conclusions

Gold nanoparticles with 5 nm and 10 nm diameters were self-assembled to the fibril forming peptide bamc16-22 and their assembly was studied by TEM and UV-Vis measurements. The 10 nm GNP's exhibited a larger propensity to bind to the peptide fibrils than the 5 nm GNP's, as showed in the TEM images taken to characterize their assembly and the UV-vis measurements were in agreement with the results obtained by TEM. The TEM images reveal that the 10 nm gold nanoparticles attach to the peptide beta-sheets before the mature fibril formation.

The staining with Congo red showed that the peptide exhibits the ability to form beta-sheets by itself. The fibrils formed in the presence of the 5 nm or 10 nm gold nanoparticles and stained with Congo red also consist of beta-sheets.

References

[1] Daniel, M. C.; Astruc, D. *Chem. Rev.* **2004**, 104, 293-346.

[2] Murray, C.B.; Kagan, C.R.; Bawendi, M. J. *Annu. Rev. Mater. Sci.* **2000**, 30, 545-610.

[3] Busbee, B.D.; Obare, S. O.; Murphy, C. J. *Adv Mater.* **2003**, 15, 414-416.

[4] Sun, Y. G.; Xia, Y. N. *Science*, **2002**, 298, 2176- 2179

[5] Pima, N.; Weiss, K.; Urban, J.; Pileni, M. P. *Adv. Mater.* **2001**, 13, 261-264.

[6] Hartgerink, J. D.; Beniashi, E.; Stupp, S. I. *Science*, **2001**, 294, 1684-1688.

[7] Lu, K.; Jacob, J.; Thiyagarajan, P.; Conticello, V. P., Lynn, D. G. *J. Am. Chem. Soc.*, **2003**, 125,6391-6393.

[8] Reches, M.; Gazit, E. *Science*, **2003**, 300, 625-627.

[9] Rajagopal, K.; Schneider, J. P. *Cur. Opin. Struct. Biol.*, **2004**, 14, 480-486.

[10] Petkova, A. T.; Leapman, R. D.; Guo, Z.; Yau, W.; Mattson, M. P.; Tycko, R. *Science*, **2005**, 307, 262-265.

[11] Tjrenberg, L. O.; Naslund, J.; Lindqvist, F.; Johansson, J.; Karlstrom, A. R.; Terenius, L.; Nordstedt, C. *J. Biol. Chem.*, **1996**, 271, 8545-8548.

[12] Tycko, R. *Cur. Opin. Struct. Biol.*, **2004**, 14, 96-103.

[13] Torok, M.; Milton, S.; Kayed, R.; Wu, P.; McIntire, T.; Glabes, C. G.; Langen, R., *J. Biol. Chem.*, **2002**, 277, 4810-40815

[14] Tjrenberg, L. O.; Callaway, D. J. E.; Tjrenberg, A.; Hahne, S.; Lilliehook, C.; Terenius, L.; Thyberg, J.; Nordstedt, C. *J. Biol. Chem.*, **1999**, 274, 18, 12619-12625

[15] Ma, B.; Nussinov, R. *Proc. Natl. Acad. Sci. USA*, **2002**, 99, 14126-14131

[16] Klimov, D. K.; Thirumalai, D. *Structure* **2003**, 11, 295-307

[17] Chan, W. C.; White, P. D. *Fmoc Solid Phase Peptide Synthesis*, Oxford University Press, New York, **2000**, page 13-18

[18] Keren, K.; Krueger, M..; Gilad, M; Ben-Yoseph, G; Sivan, U.; Braun, E. *Science* **2002**, 297, 72-75

[19] Alexandrescu, A. T. *Protein Science* **2005,** 14, 1-12.

[20] *Colloidal Gold Principles, Methods, and Applications*, Hayat, M. A., Academic Press, Inc.:**1989,** San Diego, California, Vol. 1, page 1-3

[21] *Colloidal Gold Principles, Methods, and Applications*, Hayat, M. A., Academic Press, Inc.:**1989**, San Diego, California, Vol. 1, page 17-22.

[22] Jang, S.; Park, J.; Shin, S.; Yoon, C.; Choi, B. K.; Gong, M.; Joo, S. W. *Langmuir*, **2004**, 20, 1922-1927.

[23] Bouset, L.; Redeker, V.; Decottignies, P.; Dubois, S.; Le Marechal, P.; Melki, R. *Biochemistry*, **2004**, 43, 5022-5032

[24] Brown, A. M.; Tummolo, D. M.; Rhodes, K. J.; Hofmann, J. R.; Jacobsen, J. S.; Sonnenberg-Reines, J. *J. Neurochemistry*, **1997**, 69, 1204-1212

[25] Gray, J. J. *Cur. Opin. Struct. Biol.*, **2004**, 14, 110-115.

[26] Kaiser, E.; Colescott, R. L.; Bassinger, D. C.; Cook, P. I. *Anal. Biochem*. **1970**, 34, 595-598

[27] *Neurodegenerative Disorders: Loss of Function through Gain of Function*, Beyreuther, K., Christen, Y., Masters, C. L., Springer-Verlag Berlin Heidelberg New York: **2001**, Germany, page 97-99

[28] Bousset, L., Redeker, V., Decottiginies, P., Dubois, S., Le Marechal, P., Melki, R. *Biochemistry*, **2004**, 43, 5022-5032

[29] Reches, M., Porat, Y., Gazit, E. *J. Biol. Chem*., **2002**, 277, 38, 35475-35480

[30] Collier, C. P., Mattersteig, G., Wong, E. W., Luo, Y., Beverly, K., Sampaio, J., Raymo, F. M., Stoddart, J. F., Heath, J. R. *Science*, **2000**, 289, 1172-1175

[31] Yurke, B., Turberfield, A. J., Mills, A. P., Simmel, F. C., Neumann, J. L. *Nature*, **2000**, 406, 605-608

[32] Sasaki, S., Karube, I., *Trends Biotechnol*. **1999**, 17, 50-52

[33] Chan, W. C.; White, P. D. *Fmoc Solid Phase Peptide Synthesis*, Oxford University Press, New York, **2000**, page 65, 70-71

Vita

Maria Tanase was born in Deva, Romania. In 1992 she graduated with a BS degree from the University “Babes-Bolyai” Cluj-Napoca, Romania, and in 1999 she took a Master in Business and Administration at the same University. In 2003 she joined the University of New Orleans as a graduate student in Dr. Paul Hanson’s group. She is a member of the American Chemical Society.